Dislocation density evolution during high pressure torsion of a nanocrystalline Ni–Fe alloy

Cite as: Appl. Phys. Lett. **94**, 091911 (2009); https://doi.org/10.1063/1.3095852
Submitted: 14 January 2009 • Accepted: 17 February 2009 • Published Online: 06 March 2009

Y. B. Wang, J. C. Ho, Y. Cao, et al.

Dislocation density evolution during high pressure torsion of a nanocrystalline Ni–Fe alloy

Y. B. Wang,[1] J. C. Ho,[1] Y. Cao,[1] X. Z. Liao,[1,a)] H. Q. Li,[2] Y. H. Zhao,[3] E. J. Lavernia,[3] S. P. Ringer,[4] and Y. T. Zhu[5]
[1]*School of Aerospace, Mechanical & Mechatronic Engineering, The University of Sydney, NSW 2006, Australia*
[2]*Los Alamos National Laboratory, Los Alamos, New Mexico 87545, USA*
[3]*Department of Chemical Engineering and Materials Science, University of California at Davis, Davis, California 95616, USA*
[4]*Australian Key Centre for Microscopy & Microanalysis, The University of Sydney, NSW 2006, Australia*
[5]*Department of Materials Science & Engineering, North Carolina State University, Raleigh, North Carolina 27695-7919, USA*

(Received 14 January 2009; accepted 17 February 2009; published online 6 March 2009)

High-pressure torsion (HPT) induced dislocation density evolution in a nanocrystalline Ni-20 wt %Fe alloy was investigated using x-ray diffraction and transmission electron microscopy. Results suggest that the dislocation density evolution is fundamentally different from that in coarse-grained materials. The HPT process initially reduces the dislocation density within nanocrystalline grains and produces a large number of dislocations located at small-angle subgrain boundaries that are formed via grain rotation and coalescence. Continuing the deformation process eliminates the subgrain boundaries but significantly increases the dislocation density in grains. This phenomenon provides an explanation of the mechanical behavior of some nanostructured materials. © *2009 American Institute of Physics*. [DOI: 10.1063/1.3095852]

Dislocations play a key role in determining the mechanical properties of materials. Manipulating dislocation density and distribution via appropriate processing including annealing and cold working can therefore change the mechanical properties of materials. It has been well known that conventional coarse-grained metals and alloys can be softened by annealing and strengthened by cold working.[1] Annealing reduces the dislocation density in materials, while cold work increases the dislocation density and therefore results in work hardening. On the other hand, an increase in dislocation density by cold working reduces the capacity for further dislocation accumulation and this decreases the ductility of the materials. Interestingly, the processing-property relationships of some nanostructured materials have been reported to be fundamentally different from that of coarse-grained materials. For example, nanostructured Al can be strengthened by annealing and softened by deformation.[2] The unique processing-property relationship of nanostructured materials is considered to be closely related to the unique dislocation behavior/deformation mechanisms made possible by the nanostructuring.

The deformation mechanisms of nanostructured materials are different from that of coarse-grained materials. For example, for materials with grain sizes of tens of nanometers, partial dislocation emissions from grain boundaries play a significant role in plastic deformation.[3–6] The difference in deformation mechanisms affects the evolution of dislocation density during plastic deformation and subsequently affects the mechanical behavior of the materials. *In situ* x-ray diffraction (XRD) peak profile analysis of nanocrystalline (nc) Ni, which has an average grain size of 26 nm, under uniaxial tensile straining[7] has revealed that grain boundaries act as the source and sink for dislocations, leaving no additional dislocation debris, as predicted by molecular dynamics simulations[8] in nc grains. This leads to the absence of substantial work hardening in nc metals.[7]

Recent experimental results have demonstrated evidence for grain growth of nc metals and alloys during plastic deformation.[9–11] The grain growth occurs via grain rotation and coalescence for nc grains of the sizes of ~20 nm.[12–14] The grain rotation process results in the development of a large fraction of small-angle subgrain boundaries with a high density of dislocations located at the boundaries.[14] It is not clear how these boundary dislocations change the global dislocation behavior and subsequently affect the deformation behavior of the materials. To uncover the effect of the deformation induced grain rotation and coalescence on the global dislocation behavior in nanostructured materials, we have applied XRD peak profile analysis and high-resolution transmission electron microscopy (TEM) to investigate the evolution of dislocation density and distribution of nc Ni-20 wt %Fe disks processed by the high-pressure torsion (HPT) technique.

The as-received NiFe alloy used in this investigation was produced via electrochemical deposition.[15] Disks with a thickness around 0.7 mm and a diameter of 10 mm were processed using HPT for one and nine revolutions, respectively, under 3.8 GP at room temperature. XRD experiments were carried out using a Siemens D5000 diffractometer. Details of the XRD peak profile analysis method have been described in Ref. 16. A coarse-grained NiFe sample obtained by annealing the as-received alloy at 600 °C for 3 h followed by water quenching was used as the XRD peak broadening reference. TEM observations were carried out using a Philips CM12 microscope working at 120 kV and a JEOL 3000F microscope operating at 300 kV.

a)Author to whom correspondence should be addressed. Electronic mail: xliao@usyd.edu.au.

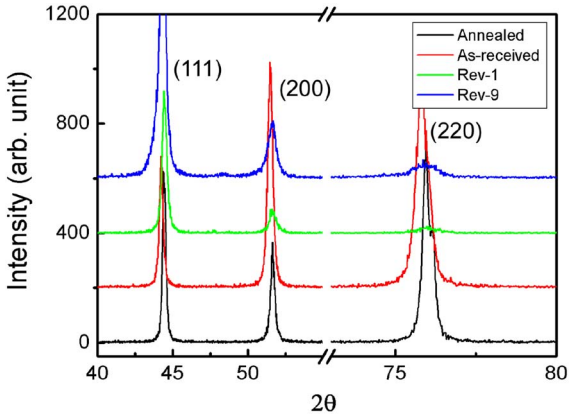

FIG. 1. (Color online) XRD patterns of the annealed (coarse-grained), as-received one-revolution HPT and the nine-revolution HPT samples.

Figure 1 shows XRD patterns of the annealed, as-received, one-revolution HPT, and the nine-revolution HPT samples. All samples are of the same face-centered-cubic structure. XRD peak profile analysis suggests that the dislocation densities in the as-received, the one-revolution HPT, and the nine-revolution HPT samples are 8.3×10^{14}, 5.7×10^{14}, and 10.2×10^{14} m^{-2}, respectively, indicating that the dislocation density *within* the grains of the NiFe alloy does not evolve monotonously but decreases initially and then increases. This dislocation density evolution process is different from that in coarse-grained materials where dislocation density increases initially and then decreases.[17] Plastic deformation induced dislocation density reduction in a nc material has recently been reported by Li *et al.*[18] during a cold rolling process. However, the latter stage of dislocation density evolution, i.e., deformation induced dislocation density increase, has never been reported. Note that the value of dislocation density calculated from XRD peak profile analysis is usually only semiquantitative. However, the trend of dislocation density evolution is valid if it is measured and analyzed in a consistent way.

The average grain size of the as-received sample is ~22 nm. The dislocation density in the as-received sample obtained from statistical analysis of high-resolution TEM images is 1.2×10^{16} m^{-2}, i.e., close to five dislocations in each grain on average. An example of a grain containing a few dislocations in the as-received sample is shown in Fig. 2. Such a high density of dislocations in nc grains is very unstable and the dislocations tend to glide to and disappear at grain boundaries when an external force is available to activate dislocation motion.[19] This is proposed as the reason for the dislocation density reduction during the initial stages of HPT of the nc Ni–Fe alloy. Statistical analysis of high-resolution TEM images suggests that the dislocation density within the grains of the one-revolution TEM sample is 6.4×10^{15} m^{-2}, which is about half of the original density.

In addition to reducing the dislocation density within grains, the HPT process also results in grain growth via grain rotation, forming larger grains that contain a large fraction of small-angle subgrain boundaries and high densities of dislocations located at the subboundaries. Figures 3(a) and 3(b) show a bright-field TEM image and a high-resolution TEM image of the one-revolution HPT sample, respectively. The grain sizes of the sample are in the range of 40–250 nm with an average grain size of ~95 nm. Atoms at the subgrain boundaries are rearranged and high densities of dislocations

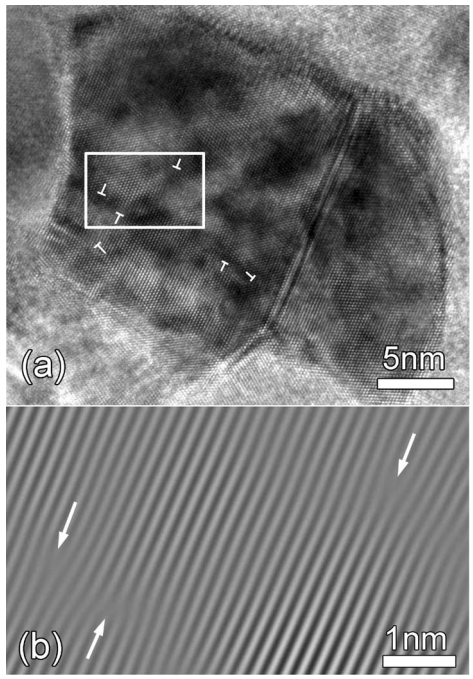

FIG. 2. (a) A high-resolution TEM image of a grain in the as-received sample. Dislocation cores are indicated using "*T*." (b) A one-dimensional Fourier-filtered image of the selected area marked in (a). Dislocation cores are indicated with arrows.

formed at the boundaries to accommodate the geometrical misorientation between neighboring subgrains. The grain boundary dislocations are clearly seen in Fig. 3(a) as dotted points and in the high-resolution TEM image in Fig. 3(b). Note that these boundary dislocations cannot be fully accounted for by XRD because dislocations located at subgrain boundaries do not produce as much elastic strain as those in the grain interior. Including the boundary dislocations increases the dislocation density in the one-revolution HPT sample to about 5.3×10^{16} m^{-2}, almost one order of magnitude higher than the density value that does not include the grain boundary dislocations.

With the development of the HPT process, the misorientation angles between neighboring subgrains decrease gradually to zero and the dislocations that accommodate the mis-

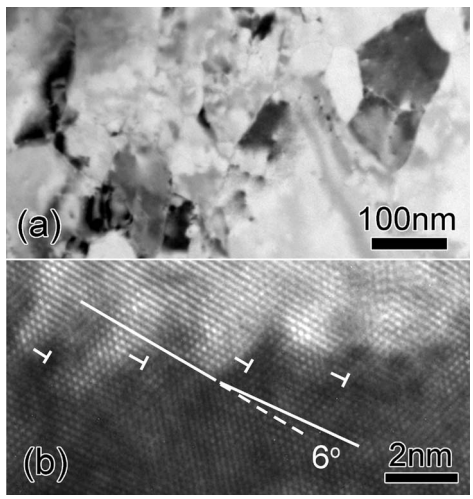

FIG. 3. (a) A bright-field TEM image of the one-revolution HPT sample. (b) A high-resolution image showing high density of dislocations, marked with "*T*," located at a subgrain boundary. The 6° misorientation between the neighboring subgrains is indicated in (b).

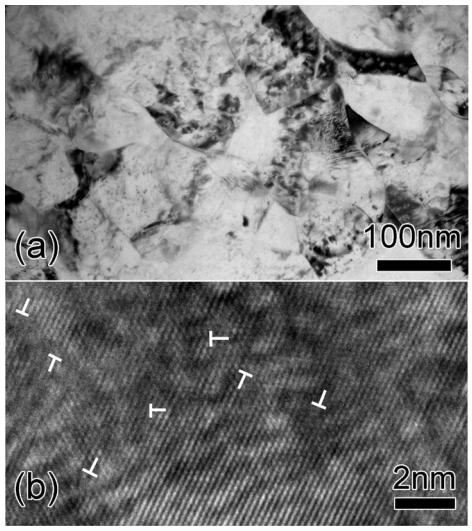

FIG. 4. (a) A bright-field TEM image of the nine-revolution HPT sample. (b) A high-resolution TEM image showing random distribution of high density of dislocations, which are marked with "*T*."

orientation necessarily glide away.[20,21] Because the subgrain boundaries exist three-dimensionally,[14] it is expected that, when boundary dislocations glide through the grains, the dislocations lying on different groups of {111} planes will interact and tangle with each other. This not only hinders the motion of dislocations but also provides sources (e.g., the Frank–Reed sources) for dislocation multiplication within grains. As a result, dislocation density in grains is expected to increase significantly. Figure 4 shows a bright-field TEM image (a) and a high-resolution TEM image (b) of the nine-revolution HPT sample. Small-angle subgrain boundaries no longer exist while random distribution of high density of dislocations is observed. The dislocation density in the grains of the nine-revolution HPT sample is $\sim 4 \times 10^{16}$ m^{-2}, which is more than six times higher than the dislocation density within the grains of the one-revolution sample but is compatible to the density in the one-revolution HPT sample if dislocations at subgrain boundaries are included.

Note that all the dislocations seen in Fig. 4 are full dislocations (partial dislocations are always associated with stacking faults), suggesting that the mechanism of partial emissions from grain boundaries does not play an observable role during the deformation process here. The high density of full dislocations seen in Fig. 4 could be generated from both grain interior and grain boundaries.

It was reported that the deformation behavior of a nc Ni–Fe alloy is a function of applied strain;[22] at low strains, deformation is mainly accommodated at grain boundaries, while at high strains, dislocation motion dominates. This phenomenon is consistent with our observations. At the initial stage of deformation, two phenomena were observed: (1) dislocation density within nc grains decreases, suggesting that there is no dislocation multiplication and that dislocations do not play any significant role in the deformation, and (2) grain growth occurs through grain rotation and atomic rearrangement at small-angle subgrain boundaries, indicating that the grain boundaries play a significant role at this stage of deformation. Further deformation reduces the misorientation angles between neighboring subgrains and forces the subgrain boundary dislocations to glide away along different groups of {111} planes, resulting in dislocation tangling that provides additional sources for dislocation multiplication. The dislocation interaction at the later stage of deformation significantly increases both the dislocation density and the dislocation storage capability and, therefore, significantly increases the strength while at the same time retaining the ductility of the materials.[22]

In summary, our structural investigation of a nc Ni–Fe alloy at different stages of the HPT process reveals that the deformation induced dislocation density evolution in the material is different from that in coarse-grained materials. Briefly, the dislocation density within grains initially decreases and then increases with increasing HPT strain.

The authors are grateful for scientific and technical input and support from the Australian Microscopy & Microanalysis Research Facility node at the University of Sydney. This project is supported by the Australian Research Council [Grant No. DP0772880 (Y.B.W., J.C.H, Y.C., and X.Z.L.)], the LDRD program of Los Alamos National Laboratory (H.Q.L.), Office of Naval Research [Grant Nos. N00014-04-1-0370 and N00014-08-1-0405 (Y.H.Z. and E.J.L.)], and the U.S. DOE IPP Program (Y.T.Z.).

[1] W. D. Callister, Jr., *Materials Science and Engineering: An Introduction* (Wiley, New York, 2007), pp. 191–199.
[2] X. X. Huang, N. Hansen, and N. Tsuji, Science **312**, 249 (2006).
[3] X. Z. Liao, F. Zhou, E. J. Lavernia, S. G. Srinivasan, M. I. Baskes, D. W. He, and Y. T. Zhu, Appl. Phys. Lett. **83**, 632 (2003).
[4] X. Z. Liao, Y. H. Zhao, S. G. Srinivasan, Y. T. Zhu, R. Z. Valiev, and D. V. Gunderov, Appl. Phys. Lett. **84**, 592 (2004).
[5] V. Yamakov, D. Wolf, S. R. Phillpot, and H. Gleiter, Acta Mater. **50**, 5005 (2002).
[6] H. Van Swygenhoven, Science **296**, 66 (2002).
[7] Z. Budrovic, H. Van Swygenhoven, P. M. Derlet, S. Van Petegem, and B. Schmitt, Science **304**, 273 (2004).
[8] V. Yamakov, D. Wolf, S. E. Phillpot, A. K. Mukherjee, and H. Gleiter, Nature Mater. **1**, 45 (2002).
[9] K. Zhang, J. R. Weertman, and J. A. Eastman, Appl. Phys. Lett. **87**, 061921 (2005).
[10] X. Z. Liao, A. R. Kilmanetov, R. Z. Valiev, H. S. Gao, X. D. Li, A. K. Mukherjee, J. F. Bingert, and Y. T. Zhu, Appl. Phys. Lett. **88**, 021909 (2006).
[11] G. J. Fan, L. F. Fu, H. Choo, P. K. Liaw, and N. D. Browning, Acta Mater. **54**, 4781 (2006).
[12] Z. W. Shan, E. A. Stach, J. M. K. Wiezorek, J. A. Knap, D. M. Follstaedt, and S. X. Mao, Science **305**, 654 (2004).
[13] Y. B. Wang, B. Q. Li, M. L. Sui, and S. X. Mao, Appl. Phys. Lett. **92**, 011903 (2008).
[14] Y. B. Wang, J. C. Ho, X. Z. Liao, H. Q. Li, S. P. Ringer, and Y. T. Zhu, Appl. Phys. Lett. **94**, 011908 (2009).
[15] H. Q. Li and F. Ebrahimi, Mater. Sci. Eng., A **347**, 93 (2003).
[16] Y. H. Zhao, Z. Horita, T. G. Langdon, and Y. T. Zhu, Mater. Sci. Eng., A **474**, 342 (2008).
[17] F. Dalla Torre, R. Lapovok, J. Sandlin, P. F. Thomson, C. H. J. Davies, and E. V. Pereloma, Acta Mater. **52**, 4819 (2004).
[18] L. Li, T. Ungár, Y. D. Wang, G. J. Fan, Y. L. Yang, N. Jia, Y. Ren, G. Tichy, J. Lendvai, H. Choo, and P. K. Liaw, Scr. Mater. **60**, 317 (2009).
[19] Z. W. Shan, R. K. Mishra, S. A. S. Asif, O. L. Warren, and A. M. Minor, Nature Mater. **7**, 115 (2008).
[20] S. V. Bobylev, M. Yu. Gutkin, and I. A. Ovid'ko, Acta Mater. **52**, 3793 (2004).
[21] A. J. Haslam, S. R. Phillpot, D. Wolf, D. Moldovan, and H. Gleiter, Mater. Sci. Eng., A **318**, 293 (2001).
[22] H. Q. Li, H. Choo, Y. Ren, T. A. Saleh, U. Lienert, P. K. Liaw, and F. Ebrahimi, Phys. Rev. Lett. **101**, 015502 (2008).